Journal of Chromatographic Science, 2019, Vol. 00, No. 00, 1–14
doi: 10.1093/chromsci/bmz116
Article

Article

Simultaneous Pharmacokinetics Estimation of Nateglinide and Pioglitazone by RP-HPLC: Computational Study to Unlock the Synergism

Suddhasattya Dey[1], Souvik Basak[1,*], Anjan De[1,*], Shahreja Parvez[1], Tabassum Hossain[2], Achintya Saha[2], Manik Ghosh[3] and Tanushree Karmakar[1]

[1]Dr. B.C. Roy College of Pharmacy and Allied Health Sciences, Bidhan Nagar, Durgapur, West Bengal 713206, India [2]Department of Chemical Technology, University of Calcutta, Kolkata, West Bengal 700009, India [3]Department of Pharmaceutical Sciences and Technology, Birla Institute of Technology, Mesra, Ranchi, Jharkhand 835215, India

*Author to whom correspondence should be addressed. Email: souvik_basak1@yahoo.com (S.B.); E-mail: de.anjan@yahoo.co.in (A.D.)

Received 5 July 2018; Revised 12 November 2019; Editorial Decision 17 November 2019; Accepted 23 November 2019

Abstract

Nateglinide (NAT) and Pioglitazone (PIO) are an antidiabetic drugs combination and currently under clinical trial in countries like Japan. In this study, an alternative, a simple, sensitive high-performance liquid chromatography method has been developed (limit of detection: 15 ng/mL and limit of quantification: 50 ng/mL) for simultaneous estimation of this drug combination in rat plasma. Most remarkably, bioavailability of NAT has been increased markedly on coadministration with PIO, than when it was administered alone. Thus, PIO is assumed to retard the catabolism of NAT by inhibiting metabolic liver-microsomal enzyme, especially CYP2C9. Using a Waters Nova-Pak C $_{18}$ column (150 $\times$ 3.9 mm, 4 μm) and a mobile phase of acetonitrile: 10 mM KH_2PO_4 (60: 40, V/V (volume by volume)) pH 3.5, the analysis was performed at 210 nm with a flow rate of 1.5 mL/min. *In silico* docking *via* molecular dynamics simulation revealed that NAT-CYP2C9 binding affinity may be reduced after PIO attachment, presumably due to the binding site overlapping of the two drugs. Thus, it has been proposed that NAT and PIO may be an efficient synergistic fixed dose combination against diabetes mellitus, and the above method can foster a simple but highly sensitive bioanalytical estimation for routine analysis.

Introduction

Nateglinide (NAT), chemically (N(trans-4-isopropyl cyclohexyl carbonyl)-d-phenylalanine), d-phenylalanine derivative, neither a sulfonylurea or benzamido moiety, is a novel oral mealtime glucose regulator and approved for the treatment of type-2 diabetes mellitus recently (1, 2). Pioglitazone (PIO) hydrochloride, (9)-5-{4-(2-(5-ethyl-2-pyridyl) ethoxy) benzyl}-2,4-thiazolidinedione hydrochloride salt, is also an oral antidiabetic agent that has been shown to affect abnormal glucose and lipid metabolism associated with insulin resistance by enhancing insulin action on peripheral tissues in animal models (3–7). The NAT works by stimulating the β-cell membrane of the pancreas to release insulin after closing the ATP-dependent potassium channels, which leads to an opening of the calcium channels. The resulting influx of calcium induces insulin secretion. It is rapidly and completely absorbed from the gastrointestinal tract, and peak plasma concentration reaches at 0. 5–1.0 hours. It is metabolized by cytochrome P-450 system to inactive metabolite and eliminated with a half-life of 1.4 hours (8). The PIO is extensively metabolized by hydroxylation and oxidation. Metabolites M-III (keto derivative of PIO) and M-IV (hydroxy derivative of PIO) are pharmacologically actives in animal models of type 2 diabetes. At steady-state, M-III and M-IV reach serum concentrations equal to or greater than PIO (9). Due to increased insulin resistance by

administration of NAT alone, it is recommended to use the drug with thiazolidones in order to affect glucose metabolism by increasing insulin sensitivity of the associated cells. Hence, NAT with PIO has gained attraction in recent combination drug development, and as a result, this dual drug regimen has been under clinical trial in Japan for last few years against type-II diabetes mellitus.

In the concurring demand for method development of this budding drug combination both *in* and *ex-vivo*, earlier reports demonstrated some methods for determination of each analyte either *in* or *ex-vivo*. However, no report is available till date about simultaneous determination of the analytes together with their combined pharmacokinetics. For example, several analytical methods have been developed for the separation and quantification of NAT from different matrices. Ono *et al*. illustrated the estimation of NAT and its main metabolites (10, 11) with column switching high-performance liquid chromatography (HPLC) after solid phase sample preparation. Ho *et al*. detected 10 antidiabetic drugs, including NAT from equine plasma and urine by liquid chromatography–tandem mass spectroscopy (LC-MS) (12). The NAT has been successfully quantified in animal plasma by Yan *et al*. using micellar electrokinetic chromatography and on-line sweeping technique (13). Analysis of PIO and its metabolites in biological fluids by HPLC with ultraviolet detection (LC-UV) has appeared in the literature (14–16). However, previously published HPLC assays lack specificity, sufficient sensitivity (limit of quantification [LOQ]: 10–50 ng/mL using a sample volume of 0.2–0.5 mL) and require long analytical run times (over 20 minutes), which make the LC-UV method impractical for routine analysis for large numbers of clinical samples. Quantitative LC-MS/MS describes a sensitive, specific and rapid method for the simultaneous determination of PIO and its two active metabolites (M-III and M-IV) in human plasma (17). Yin *et al*. have studied chiral separation of NAT and its l-enantiomer on monolithic molecularly imprinted polymers (18). Detection of metformin and NAT from human plasma by cation exchanging with normal-phase LC/MS has been reported (19). Recently, reverse phase HPLC method has been reported for the determination of NAT in rabbit plasma (20). In light of this, we have tried to develop an alternative HPLC method for such drug–drug interactions, which may be routinely operated day to day for in-house laboratory techniques. This present work presents a highly sensitive HPLC method for simultaneous determination of NAT and PIO in rat plasma despite several attempts that have been performed earlier to estimate pharmacokinetics of those drugs in various fixed dose combinations (FDCs). (21–22)

Nowadays, it is well-known fact that synergistic drug action in combination therapy may increase the bioavailability of parent drug/s compared with that of its solitary administration. Earlier literature based on isolated enzyme kinetics reported that PIO reduces NAT conversion to its metabolites especially M-I (23) by inhibiting liver microsomal CYP2C9 and CYP3A4, which are major metabolizing enzymes of NAT (24, 25) Thus, pharmacokinetics study, which has not yet been reported for this drug combination, has been undertaken in this work. We propose that it can provide a new insight for designing dosage form together with a promising novel approach in antidiabetic therapy.

Material and Methods

Reagents and chemicals

The NAT (Figure 1A) was generously gifted by Dr. Reddy's Lab. Ltd, Hyderabad, and PIO. hydrochloride (Figure 1B) was obtained as a gift sample from Lupin Ltd, Goa. The HPLC grade solvents, such as acetonitrile, methanol and water together with analytical grade reagents, such as perchloric acid, orthophosphoric acid (85%) and dihydrogen phosphate buffer, were obtained from Merck Specialties Private Limited, Worli, Mumbai, India. Male Swiss Albino rats (200~220 g) was used for the animal study involving *in vitro* metabolism study on liver microsomal enzymes. For general buffering of cell lysate and enzymes, phosphate buffer (pH 7.0) was used.

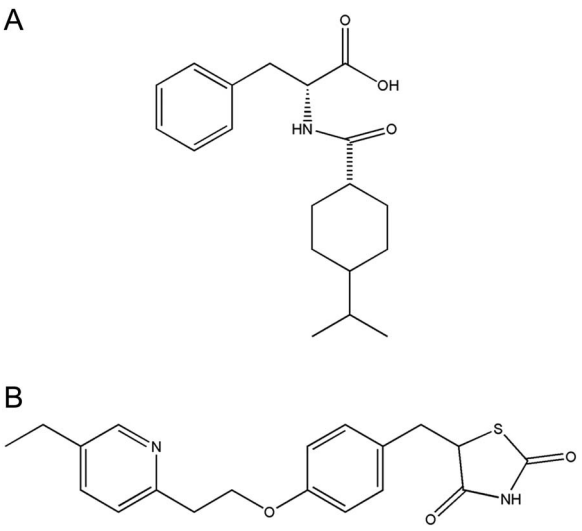

Figure 1. Chemical structures of compounds. (A) NAT. (B) PIO.

Preparation of stock and standard solutions

Stock solution of NAT and PIO of 1 mg/mL was prepared in methanol. Standard solutions of NAT and PIO were prepared by diluting the appropriate amounts of the individual stock solution using methanol. Standard solutions were prepared in the range of 100–2000 µg/mL for NAT and 25–500 µg/mL for PIO. Stock solutions were refrigerated when not in use and replaced on a weekly basis. Fresh standard solutions were prepared for each day of analysis for validation.

Chromatography

The HPLC (Waters Isocratic System, USA) system was composed of a pump (Model no. 515) with solvent delivery module, having manual rheodyne injector with a 20-µL fixed loop and with a UV-VIS detector (Model no. 2489). Throughout the study, the analytical wavelength was set at 210 nm. Analytes were separated by using Waters Nova-Pak C18 Column (column length 150 × 3.9 mm, 4 µm particle size) at an ambient temperature. The data acquisition was made with Software-M-power. Isocratic elution was followed with a mobile phase of acetonitrile: 10 mM KH_2PO_4 (60:40, V/V), pH 3.5 (adjusted with 10% orthophosporic acid). The mobile phase flow rate was set at 1.5 mL/min.

Sample collection

Use of animals in this study was approved by The Committee for the Purpose of Control and Supervision on Experimental Animals. Regn. No BCRCP/IAEC/8/2014). The rats were housed one animal per cage at Animal House of Dr. B. C. Roy College of Pharmacy and Allied

Health Sciences, Durgapur, West Bengal, India. The temperature and relative humidity were maintained at 22 ± 2°C and 50 ± 5%, respectively. The animals were controlled with daily food and water as directed by CPCSEA guidelines.

Blood sample (0.2 mL) of the healthy albino rats (weighing 150–250 g) was collected from veins with a 2 mL heparinized-coated micro-centrifuge tube from retro orbital plexus of albino rats. The sample was centrifuged at 24,000 g for 15 minutes, and the plasma was collected carefully. The collected plasma was stored in −20°C until further used. The blood sample was collected on a regular basis from different rats.

Sample preparation

The plasma samples were treated with protein precipitating agent for estimation of NAT and PIO in blood. Different protein precipitating agents were used (26–28). It was found that 8.25% of perchloric acid gave a clear chromatogram without any interference with NAT and PIO. The samples were centrifuged at 24,000 g for 15 minutes, and 20 µL of clear supernatant was injected through the rheodyne injector to HPLC column for analysis. The proposed method was validated as per the Centre for Drug Evaluation and Research (CDER, affiliated by Food and Drug Administration, USA) guidelines (29–31).

Linearity

The linearity was tested in the concentration range of 200, 40, 30, 20 and 10 µg/mL for NAT, whereas 50, 10, 7.5, 5 and 2.5 µg/mL for PIO. The calibration curve was constructed and evaluated through estimation of coefficient of regression (r^2).

Accuracy

Accuracy was determined by replicate analysis. Five sets of plasma samples were spiked with three different concentrations, each for NAT and PIO. Accuracy was estimated by ascertaining the differences between loaded concentrations of drugs and concentrations obtained from the peak area emulated by the proposed method.

Precision

The precision of the method is based on within-day repeatability and day-to-day reproducibility, which was determined by the replicate analysis. Plasma were spiked in the same manner as described in the "accuracy" section. Relative standard deviation (RSD) was calculated from the ratio of standard deviation to the mean and expressed in percentage. RSD within a day was calculated as Intra-day precision, and RSD in different days was calculated as Inter-day precision.

Recovery

Recovery studies were performed by estimating sample concentrations from peak height of the elutes and hence calculating the percentage recovered with respect to the concentration loaded during plasma spikings. The analysis was carried out in triplicates at 10 and 200 µg/mL for NAT and 2.5 and 40 µg/mL for PIO.

Selectivity, stability and quality control

Selectivity is a method to verify by checking for interferences of various drugs and their metabolites of the same categories. Stability was assessed by placing spiked plasma samples of different concentration at −20°C freezer (Remi, Maharashtra, India) for 6 months. Quality control (QC) was performed by analyzing the purity of each plasma peak generated from the pure drug samples after mixing in blank plasma. The details of these methods have been provided in supplementary information.

LOQ

LOQ is an assay procedure to estimate the lowest concentration of NAT and PIO (spiked plasma sample), which gives rise to a peak height thrice the baseline noise at a sensitivity of 0.005 aufs (absorbance unit full scale), which is evaluated in this study for 200 µL of the sample.

Application of the method to biological samples

This method was then applied to the pharmacokinetic study of NAT and PIO in 10 healthy albino rats. The sample preparation and HPLC evaluation have been performed as mentioned before.

Graphs were plotted for NAT and PIO (time *vs* observed plasma concentration), which emulated area under curve (AUC), calculated by the linear trapezoidal rule in Phoenix WinNonlin® software (WinNonlin®, Certara USA). The maximum observed NAT and PIO concentration (C_{max} NAT and C_{max} PIO) together with the time at which C_{max} was observed (T_{max} NAT and T_{max} PIO) and reported directly from the graph.

In vitro metabolism studies

In vitro metabolism studies were performed involving individual drugs as well as their combination in rat liver microsomal enzymes. Since performing this experiment on human beings or any human organs at institute level is prohibited according to regulatory guidelines (Agencies and guidelines restricting experimentation on human subjects-Food and Drug Administration; World Health Organization; Federal Policy for the Protection of Human Subjects, or the Common Rule (45 CFR 46); Nuremberg code; National Institute of Health, https://www.ncbi.nlm.nih.gov/books/NBK215883/ref), we have performed the drug–drug interactions by liver microsomal enzymes using rat liver. It is noteworthy that as per animal ethical guidelines, rat model is considered as an alternative to human model (https://www.genetargeting.com/crispr/the-advantages-of-rat-models/ Accession date 18/08/2019).

Preparation of cell lysate . The animals were sacrificed, their livers were taken out and immediately dipped into ice-cold phosphate buffer, pH ∼7.0. The livers were then chopped into small pieces and homogenized in tissue homogenizer with standard shearing in ice-cold condition. The homogenized mixture was centrifuged for 10 minutes at 24,000 *g* at 4°C. The supernatant was collected and subsequently was stored at 4 °C for further studies. During microsomal studies, the cell lysate was diluted suitably to obtain a uniform protein homogenate and subjected with individual drugs or combination in buffered system to measure kinetic changes on the latters. The protein estimation was performed as per Bradford Assay as described earlier (32).

Estimation of NAT-PIO Interaction . The NAT-PIO interaction was measured by standard enzyme kinetics method where liver microsomal enzymes play a major role in substrate-product conversion. The 3 mL reaction system comprised of 50 µL of diluted cell lysate, 1 mM drug solution either individually or in combination within a vehicle of phosphate buffer (pH 7.0). The mixture was then checked

Table I. Spectral and Statistical Data for Determination of NAT and PIO by Proposed HPLC Method

Parameters	Value for NAT	Value for PIO
Absorption maxima, λ_{max} (nm)		
Linearity range (µg/mL)	10–200	2.5–50
Coefficient of determination (r^2)	0.9956	0.9993
Correlation coefficient (r)	0.9977	0.9996
Regression equation (Y[a])	Y = 1054.3768x + 51,419.7920	Y = 10,725.2928x + 66,058.4080
Slope (b)	1054.3768	10,725.2928
Intercept (a)	51,419.792	66,058.408
LOD (µg/mL)	0.0151	0.0151
LOQ (µg/mL)	0.05	0.05

[a] Y = mX + C, where X is the concentration (µg/mL).

for absorbance change at 210 nm for a time range of 40 seconds. Their individual reaction rates were then calculated based on change in absorbance per second which was further normalized with per mg of protein subjected in the reaction.

Molecular docking studies

Investigation of protein and ligand interaction is known as the molecular docking study. Molecular docking studies was performed to dissect the binding chemistry of NAT and PIO with CYP2C9. Since the experimental pharmacokinetics revealed that bioavailability of NAT has been improved due to PIO inhibition of CYP2C9 (21), we investigated binding of both the drugs with CYP2C9 and evaluated if there is a possible chance of interaction between the two drugs during binding. In order, we have first performed docking of solitary NAT with CYP2C9 and evaluated the binding affinity thereof. Afterwards, the binding chemistry of PIO was evaluated by solitary PIO-CYP2C9 docking, and any conformational alteration of the protein, its binding motif or region specificity of the PIO-amino acid bonds were solved by molecular dynamics (MD) simulation of docked PIO-CYP2C9 complex. Afterwards, NAT was re-docked on to stable PIO-CYP2C9 conjugate (obtained *via* MD simulation) to evaluate any change of binding affinity after PIO binding. The docking analysis was performed on the basis of structural resolution (2.45 Å) of the crystalline CYP2C9 enzyme (PDB ID: 4NZ2) (33).

NAT and PIO docking with isolated CYP2C9 . With the structure of CYP2C9, which was downloaded from protein data bank (PDB ID: 4NZ2), docking was performed. Docking has been determined by "Glide" in Schrodinger using *Grid-Based Ligand Docking* (34). For validation of the docking method, self-docking was performed where the bound ligand was re-docked at the active site of the protein. Conformer of the original bound ligand was superimposed to the docked poses for calculation of root mean square deviation (RMSD). The docking procedure was validated by the low RMSD (<2 Å) value of original bound ligand (35). "Protein preparation wizard" module was used for preparation of protein molecule (36). At the beginning of protein preparation, hydrogen atoms were added, missing loops and atoms were added, energy was minimized and then optimized by OPLS2005 force field. With the help of "PROPKA", the protonation states were assessed (37, 38) at physiological pH 7.4. During protein preparation, the water molecules were preserved up to 5 Å around the active site, and rest were deleted. For the ligand preparation, LigPrep module (39) was used. Based on the active site of protein, the grid was generated after ligand and protein preparation. In order to enclose the receptors within 3 Å from the central domain of the residues, the grid-enclosing box was centered to the catalytic sites of the respective 3D-conformation of the receptor. Finally, with Glide XP mode docking calculation has been performed for the allocated binding site (40) that establishes all possible orientation for each low-energy conformer.

MD . MD simulation method analyzed protein residues responsible for binding to the ligand and the interactions pattern between them. The MD study provides information regarding thermodynamically stable conformation of the specific protein. "Desmond Molecular Dynamics" module (41) of Schrodinger Maestro provides an idea about the stability of protein-ligand complexes (42) utilizing OPLS2005 molecular mechanics force field. For simulation of MD, the ligand-protein complex was solvated with TIP3P water model (41). For avoiding the direct association of protein complex with its own periodic image, the orthorhombic boundary box at 10 Å was designed. Calibration of the system was done by setting other parameters kept as default. The MD simulation was carried out for 30 ns at Nose-Hoover chain thermostat at 300 K, Martyna-Tobias-Klein barostat at 1.013 bar pressure and at time step of 10 fs. In order to cross-check the stability of model system, the RMSD, root mean square fluctuation (RMSF), radius of gyration (Rg) and H-bonds were checked (42). For analysis of MD trajectory equilibration, RMSD happens to be an essential parameter, while RMSF characterizes the local changes throughout the protein chain.

NAT docked with CYP2C9-PIO complex stabilized by MD simulation. The NAT was re-docked onto CYP2C9-PIO complex stabilized by MD simulation using the same method as described above. The docked score was considered to evaluate any change in binding affinity of NAT after PIO docked onto the same.

Results

Chromatographic separation

An HPLC was used to investigate and optimize the separation of NAT and PIO. The retention time for NAT and PIO were 1.4 and 1.1 minutes in the chromatographic conditions mentioned in Material and Method section.

Linearity

The linearity was tested by plotting linear regression equation using the method of least squares through Microsoft Excel® program. The

Table II. Inter-day ($n = 5$) Precision (%RSD) Measured for QC Points for NAT in Plasma

		Day 1		Day 2		Day 3	
Plasma	TC µg/mL	EC NAT	%RSD NAT	EC NAT	%RSD NAT	EC NAT	%RSD NAT
1	200	200.679	0.271	201.151	0.189	200.818	0.216
2	30	29.208	2.107	29.818	1.285	30.082	1.015
3	10	9.719	1.293	10.187	6.954	10.038	2.745

EC, experimental concentration; TC, theoretical concentration.

Table III. Intra-day ($n = 5$) Precision (%RSD) Measured for QC Points for NAT in Plasma

		Intra-day	
Plasma	TC µg/mL	EC NAT	%RSD NAT
1	200	200.607	0.426
2	30	29.818	1.952
3	10	10.127	3.936

EC, experimental concentration; TC, theoretical concentration.

Table IV. Inter-day ($n = 5$) Precision (%RSD) Measured for QC Points for PIO in Plasma

		Day 1		Day 2		Day 3	
Plasma	TC µg/mL	EC PIO	%RSD PIO	EC PIO	%RSD PIO	EC PIO	%RSD PIO
1	50	50.972	1.188	50.516	0.887	50.707	0.982
2	7.5	7.576	3.024	7.331	0.701	7.360	1.693
3	2.5	2.241	5.385	2.245	7.428	2.269	2.646

EC, experimental concentration; TC, theoretical concentration.

correlation coefficient (r^2) was found to be 0.998 and 0.999 in rat plasma for NAT and PIO, respectively, which establishes a strong linear relationship between the variables. The detailed linearity result has been summarized in Table I.

Precision

Inter-day and intra-day precision was measured in terms of %RSD. The %RSD was found to be 1.786 and 2.105 for NAT, and 2.659 and 1.522 for PIO, which was well inside the limit according to CDER guidance for Bio-analytical Method Validation. The results of the precision analysis are summarized in Tables II, III, IV and V for NAT and PIO, respectively.

Accuracy

Accuracy study was performed according to the CDER guidelines, which was found to be 99.009–101.273 and 90.071–101.463% for NAT and PIO, respectively (Tables VI and VII), that indicated there was no interference of endogenous plasma components.

Recovery

The mean recovery of the NAT and PIO spiked plasma samples within the concentration range of 10–200 and 2.5–50 µg/mL was found to be more than 90%. The result in the recovery of NAT and PIO from spiked plasma sample was nearly 90%, which indicated lack of interference from the sample preparation procedure.

Selectivity

Selectivity of the chromatographic separation was performed to check that whether there had been any interferences due to endogenous peaks of plasma, in Figures 2A and B. The chromatograms for blank plasma (Figure 2A) and spiked plasma with NAT (40 µg/mL) and PIO (10 µg/mL) (Figure 2B) revealed that blank plasma (R_t = 0.642) does not overlap with NAT or PIO (R_t = 1.4 and 1.1 minutes, respectively) peaks with concomitant observation, even the drugs do not interfere with each other either.

Specificity

In specificity, it was observed that there was no interference or overlapping of peaks due to endogenous plasma components. Due to the presence of endogenous plasma components which resulted in peaks within 0–1 minutes, no contamination of drug peaks was observed (Figure 2B). After 1 minute, there was no significant interference of blank plasma that could affect the response of NAT and PIO.

Limit of quantification

The LOQ for NAT and PIO in rat plasma was found to be 0.05 µg using 200 µL plasma.

Stability

Mean deviation (%) was measured for three different concentrations for a time period of 1, 2, 4 and 6 months, which varied between

Table V. Intra-day (n = 5) Precision (%RSD) Measured for QC Points for PIO in Plasma

		Intra-day	
Plasma	TC µg/mL	EC PIO	%RSD PIO
1	50	50.141	1.021
2	7.5	7.340	1.062
3	2.5	2.320	2.483

EC, experimental concentration; TC, theoretical concentration.

Table VI. Summary of Inter-day (n = 5) and Intra-day (n = 5) Precision and Accuracy of the Method in Rat Plasma for NAT

Nominal concentration (µg/mL)	Mean concentration found[a] (µg/mL) NAT	SD NAT	Precision (%RSD) NAT	Mean accuracy[b] (%) NAT
Inter-day (n = 5)				
200	200.883	0.453	0.225	100.441
30	29.703	0.435	1.469	99.009
10	9.981	0.370	3.664	99.813
Intra-day (n = 5)				
200	200.607	0.855	0.426	100.303
30	29.818	0.582	1.952	99.393
10	10.127	0.399	3.936	101.273

[a]Average of three and six determinations at three concentration levels for inter-day and intra-day, respectively.
[b]All the mean accuracies were calculated against their nominal concentrations.

Table VII. Summary of Inter-day (n = 5) and Intra-day (n = 5) Precision and Accuracy of the Method in Rat Plasma for PIO

Nominal concentration (µg/mL)	Mean concentration found[a] (µg/mL) PIO	SD PIO	Precision (%R.S.D.) PIO	Mean accuracy[b] (%) PIO
Inter-day (n = 5)				
50	50.731	0.517	1.019	101.463
7.5	7.422	0.135	1.806	98.963
2.5	2.252	0.116	5.153	90.071
Intra-day (n = 5)				
50	50.141	0.512	1.021	100.281
7.5	7.340	0.078	1.062	97.867
2.5	2.320	0.058	2.483	92.792

[a]Average of three and six determinations at three concentration levels for inter-day and intra-day, respectively.
[b]All the mean accuracies were calculated against their nominal concentrations.

−4.067 to 8.600% and −1.373 to 4.560% for NAT and PIO, respectively (Tables VIII and IX). Freezing and thawing of NAT and PIO spiked plasma for three successive cycles did not affect the measured concentrations. The mean deviation was found to be within 0.623–3.233 and 0.573–1.947 for NAT and PIO, respectively from the theoretical value.

Validation

Each of the validation procedure was conducted by three analyses in the spiked plasma. When required, the analysis included standard curve and QC regimens. For QC study, different nominal concentrations were taken such as 10, 30 and 200 µg/mL for NAT and 50, 7.5 and 2.5 µg/mL for PIO by plasma spiking method. The assay of individual concentration was performed at the beginning as well as at end of the analytical run. All the above results were within the acceptable limit (±20% of their respective nominal values).

System suitability

The system suitability test is an important parameter of the chromatography system. This system suitability test gives the data for theoretical plates, HETP (Height Equivalent to Theoritical Plates) and resolution together with other relevant parameters which demonstrate the acceptability of the chromatographic system to pass the minimum limit of execution (43).

In this study, a system suitability test was performed according to United States Pharmacopoeia (USP). The test was on the chromatograms obtained from standard and test solutions to check above-mentioned parameters. The results were obtained from the six replicate injections of standard solutions and have been summarized in Table X.

Application of assay and analysis of specimens

The above developed method was therefore applied to quantify NAT and PIO concentration in rat plasma by pharmacokinetics analysis,

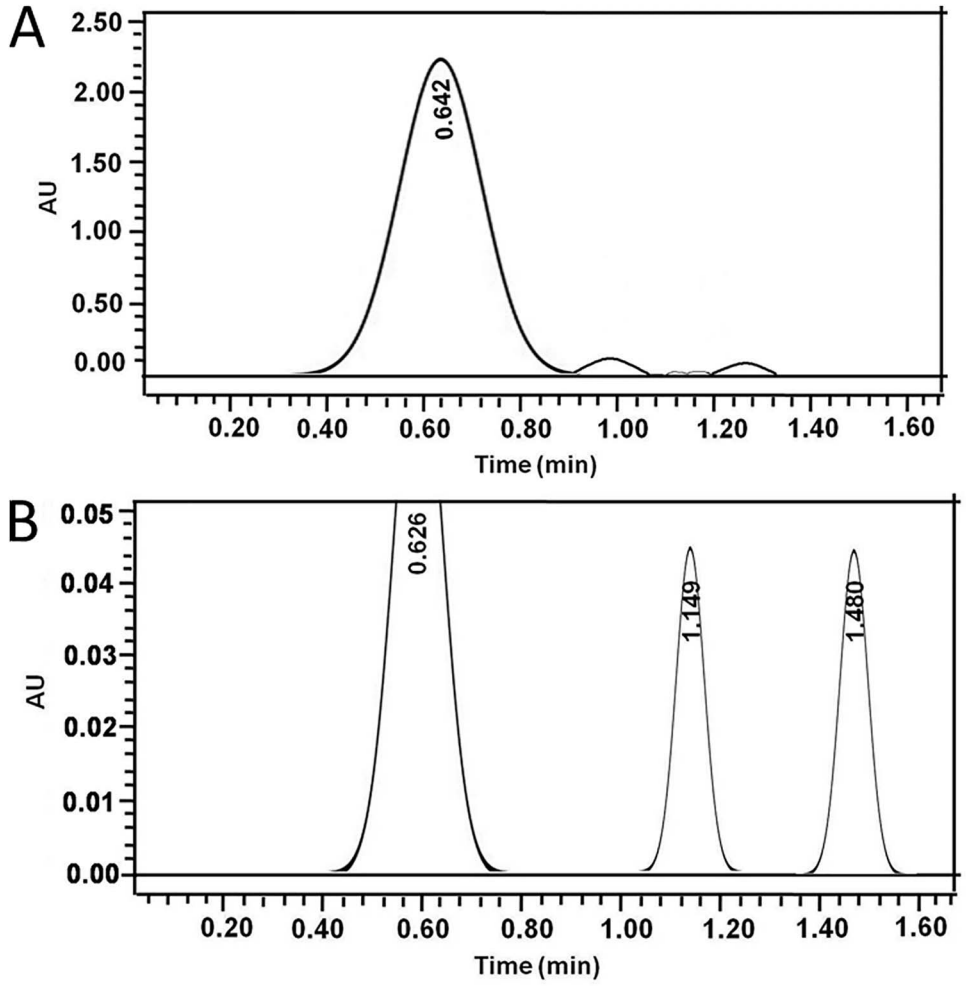

Figure 2. HPLC chromatograms for selectivity. (A) Chromatogram of blank rat plasma without NAT and PIO, (B) chromatogram of standard solution of NAT (40 µg/mL) and PIO (10 µg/mL) with retention time of 1.482 and 1.149 minutes, respectively, in rat plasma.

which was carried out on three groups of subjects, each containing 10 wistar albino rats. The HPLC chromatogram of rat plasma after 2 hours of oral drug (suspension) administration of NAT and PIO (6.16 mg/kg and 1.54 mg/kg body weight respectively) with retention times of 1.6 and 1.1 minutes has been observed (Figure 3). The elimination curve of NAT and PIO after simultaneous administration is provided in Figure 4. Different pharmacokinetic parameters were studied, which have been summarized in Tables XI and XII. The T_{max}, C_{max} and other pharmacokinetic parameters were also calculated. For NAT, the T_{max} and C_{max} have been revealed as 1.5 hours and 140.83 µg/mL, respectively, whereas for PIO, these have been estimated as 3 hours and 27.90 µg/mL in order.

In vitro liver microsomal study of NAT-PIO interaction

The individual and combined reaction rates of NAT-PIO inhibition were carried out taking each drug concentration 1 mM since an optimization study revealed that the differential metabolic conversions of individual NAT, PIO, their corresponding arithmetic sum and their mixed combination by liver extract may be explicitly depicted at this concentration (Figure 5A). Thus, the rate of reaction was expressed as ΔA/s/mg of protein taken (U) for the reaction where ΔA is the absorbance change for the reaction products between initial time (t = 0 s) and final time (t = 40s). The normalized reaction rate of NAT-PIO degradation by liver microsomal enzymes revealed that solitary NAT undergoes a metabolic conversion rate of 0.332 U, whereas solitary PIO expressed a reaction rate of 0.424 U under these conditions (Figure 5B). However, when both were co-incubated with the liver extract under the same conditions, the reaction rate was revealed as 0.309 U, which was found considerably lower than arithmetic sum of their individual reaction rates (0.896 U).

Molecular docking

Molecular docking with NAT. The docking mechanisms of NAT with the selective protein [PDB id: 4NZ2 (34)] was attempted to find out the possible binding patterns and interactions. This mechanism was analyzed using XP docking. Based on the Glide score, generated docking poses were categorized, and the best docking pose was determined by the lowest Glide score, which represents the most capable, best-fit for the ligand in the active site of the target protein. The docking interactions also compared among the NAT and respective protein 4NZ2 with the interactions present in the co-crystallized ligand. The co-crystallized ligand shows H-bond interactions with amino acids Asn107, Asn204 and Ala297 and hydrophobic interactions with Ile205, Leu208, Leu233, Val237 and Ala477. The molecular docking

Table VIII. Storage Stability Data of NAT in Plasma at Concentrations 10, 30 and 200 µg/mL

Time period (months)	Concentrations added (µg/mL)	Concentration measured (µg/mL)					
a. Long-term stability							
		Assay 1 NAT	Assay 2 NAT	Assay 3 NAT	Mean NAT	S.D. NAT	%DEV[a] NAT
1	200	202.560	202.450	202.150	202.387	0.212	1.193
	30	30.610	30.570	30.490	30.557	0.061	1.856
	10	10.910	10.890	10.780	10.860	0.070	8.600
2	200	201.890	201.560	201.670	201.707	0.168	0.853
	30	30.170	30.100	30.210	30.160	0.056	0.533
	10	10.450	10.380	10.280	10.370	0.085	3.700
4	200	200.250	200.120	200.070	200.147	0.093	0.073
	30	30.040	29.890	29.910	29.947	0.081	−0.178
	10	10.110	10.070	10.140	10.107	0.035	1.067
6	200	198.560	198.670	199.010	198.747	0.235	−0.627
	30	28.560	28.870	28.910	28.780	0.192	−4.067
	10	9.790	9.760	9.810	9.787	0.025	−2.133
b. Freeze and thaw stability							
	200	201.140	200.890	201.710	201.247	0.420	0.623
	30	30.170	30.670	30.710	30.517	0.301	1.722
	10	10.130	10.410	10.430	10.323	0.168	3.233

[a] %DEV = deviation of single mean value from theoretical value (%).
CA, concentration added; TP, time period.

Table IX. Storage Stability Data of PIO in Plasma at Concentrations 2.5, 7.5 and 50 µg/mL

Time period (months)	Concentration added (µg/mL)	Concentration measured (µg/mL)					
a. Long-term stability							
		Assay 1 PIO	Assay 2 PIO	Assay 3 PIO	Mean PIO	SD PIO	%DEV[a] PIO
1	50	52.410	52.130	52.210	52.250	0.118	4.500
	7.5	7.520	7.511	7.519	7.517	0.004	0.222
	2.5	2.560	2.574	2.553	2.562	0.009	2.493
2	50	52.340	52.520	51.980	52.280	0.224	4.560
	7.5	7.511	7.516	7.508	7.512	0.003	0.156
	2.5	2.520	2.521	2.513	2.518	0.004	0.720
4	50	51.220	51.120	51.215	51.185	0.046	2.370
	7.5	7.501	7.509	7.501	7.504	0.004	0.049
	2.5	2.510	2.507	2.507	2.508	0.001	0.320
6	50	49.780	49.180	48.980	49.313	0.340	−1.373
	7.5	7.480	7.479	7.486	7.482	0.003	−0.244
	2.5	2.489	2.465	2.471	2.475	0.010	−1.000
b. Freeze and thaw stability							
	50	50.210	50.470	51.210	50.630	0.424	1.260
	7.5	7.547	7.566	7.516	7.543	0.021	0.573
	2.5	2.514	2.561	2.571	2.549	0.025	1.947

[a] %DEV = deviation of single mean value from theoretical value (%).
CA, concentration added; TP, time period.

with NAT revealed that the drug binds with Asn217 and a water molecule of the receptor by the H-bonding and with the Phe476 by the hydrophobic interaction (Figure 6).

Molecular docking with PIO. Docking of the cytochrome P450 enzyme with PIO is depicted in Figure 7. The study revealed that the H-bond interaction can be formed with the amino acid Thr364 and PIO. Other green balloon-shaped amino acids were mainly involved for neighboring hydrophobic interactions at the active cavity site.

MD. The MD simulation was carried out for further refinement and stabilization of the docked complexes in dynamic environment using Desmond (34) to evaluate the most energetically stable binding conformation. The simulation time of 10–30 ns was used to allow and permit reorganization of the interaction configuration of protein-ligand complex. In the simulation study, we have analyzed the compactness of each simulated complex through RMSD, RMSF, Rg, the secondary structure elements of PIO ligand interactions with the selective protein along with stable H-bond and hydrophobic

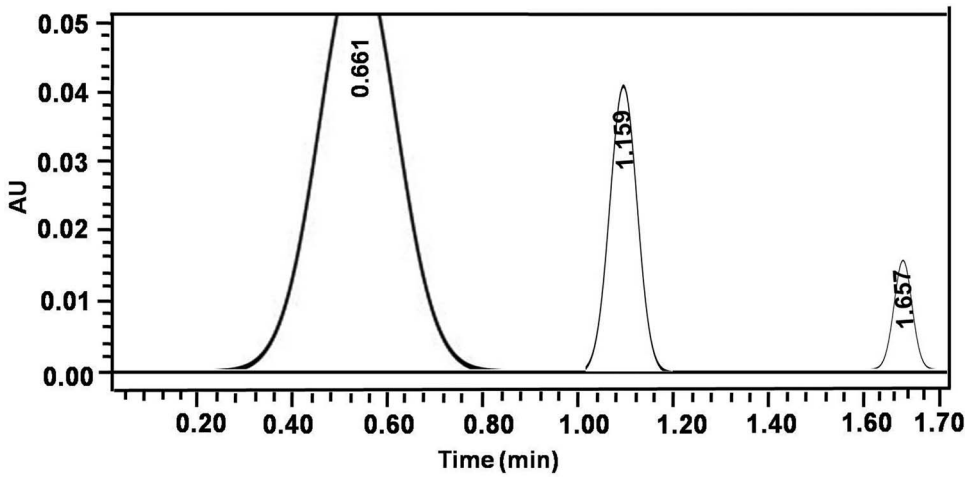

Figure 3. Chromatogram of rat plasma after 3 hours of oral administration of NAT and PIO (6.16 + 1.54) mg/kg body weight with retention times of 1.65 and 1.15 minutes for NAT and PIO, respectively, in rat plasma.

Table X. System Suitability Parameters of NAT and PIO

S. No.	Parameters	NAT	PIO
1	Retention time, Rt (minutes)	1.482	1.149
2	Capacity factor (k)	7.121	5.29
3	Separation factor (α)	1.34	
4	Theoretical plates (USP)	2756.25	2089
5	HETP (mm)	0.054	0.071
6	Resolution (Rs)	3.2	3.22

Table XI. Pharmacokinetic Parameters of NAT After a Single Oral Dose of 6.16 mg/kg and 1.54 mg/kg PIO and NAT to Three Groups Each Containing 10 Albino Rats

S. No.	Pharmacokinetic parameters	Observed value for PIO
1	Elimination rate constant, k_{el} (h^{-1})	1.3719
2	Time required for maximum plasma concentration, T_{max} (hour)	1.5000
3	Maximum plasma concentration, C_{max} (µg/mL)	140.8321
4	Plasma half-life, $T_{1/2}$ (hour)	0.5052
5	AUC at 8 hours, $AUC_{(0 \rightarrow 8)}$, (µg h/mL)	252.3918
6	AUC at infinite time, $AUC_{(0 \rightarrow \infty)}$ (µg h/mL)	252.3984
7	Area under momentum curve at 8 hours, $AUMC_{(0 \rightarrow 8)}$ (µg h^2/mL)	434.4570
8	Mean residence time, MRT (hour)	1.7214

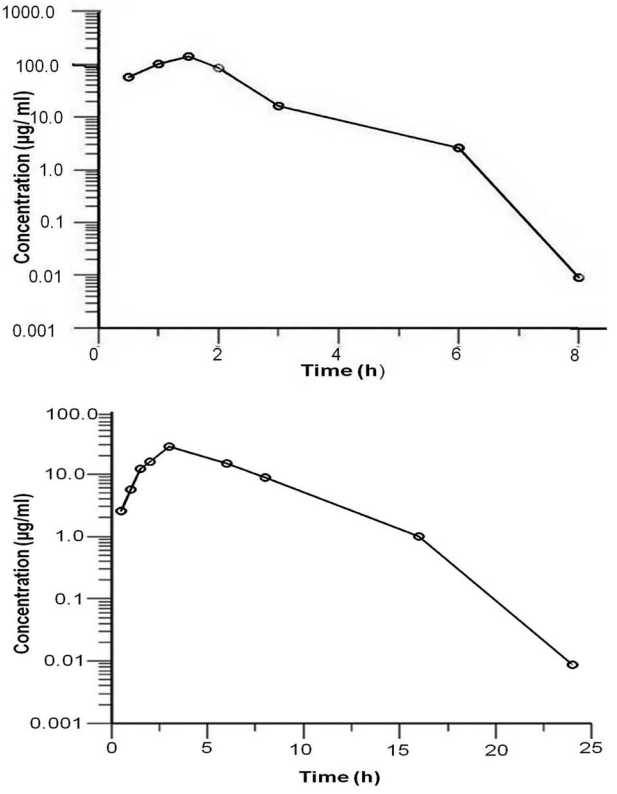

Figure 4. Natural log plasma concentrations versus time profile after oral administration of the combined dosage form (A) 6.16 mg/kg body weight of NAT (B) 1.54 mg/kg body weight of PIO.

interactions. The RMSD of the complex is analyzed (Figure 8A) through dynamic stability for both ligand and proteins. The RMSD plot of PIO (Figure 8A) shows that the complex is stable. Maximum stability has been observed at 12–30 ns. The RMSF plot is also beneficial for characterization of local alterations along with the protein chain. Analyses of RMSF graph (Figure 8B) reveal that the inhibitor has good RMSF distribution and dynamic features. Amino acids Ala106, Asn204 and Asn217 maintained stability of the protein-ligand contact during fluctuation. Therefore, the binding pocket showed adequate stability, as RMSF is limited to 4.5 Å. Residue Asn204 has Hydrogen Bonding (HB) interaction with PIO, which further changed to water-bridge bond with the ligand that confirms the stability of the complex. It maintained 40% stability of the full time length (Figure 8C). The residue Asn217 also formed HB interaction with PIO, maintained its stable interaction contact up to 93% of the time length and further changed into water-bridge bond

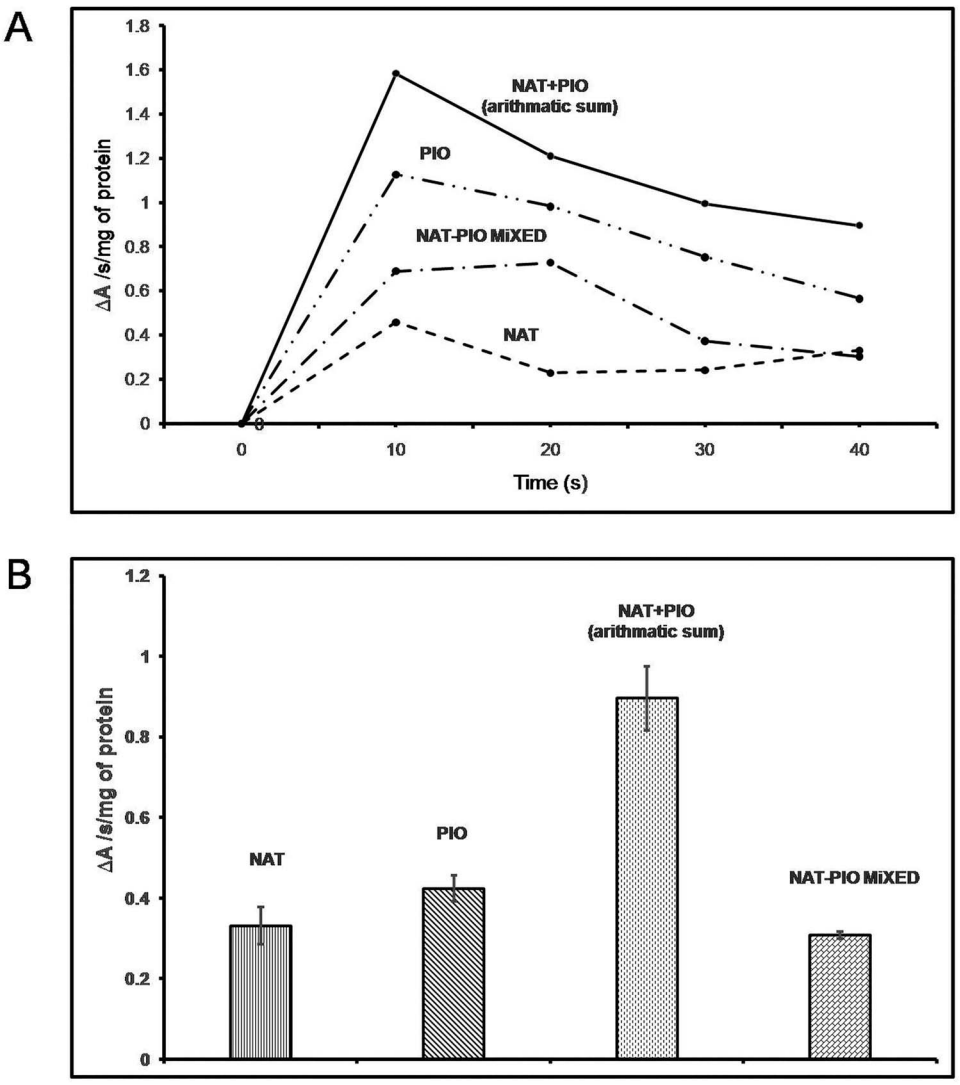

Figure 5. *In vitro* liver microsomal enzyme kinetics study of NAT and PIO. (A) Time-dependent reaction rate of solitary NAT, solitary PIO, arithmetic sum of NAT and PIO and NAT–PIO mixed cocktail with liver microsomal enzymes (involving CYP450 group of enzymes). (B) Comparive reaction rate analysis of the susbstrates with CYP450 at specific time interval (40s).

(Figure 8D). The Ala106 maintained its hydrophobic interaction that further changed to water-bridge bond. Residue Gly296 has HB interaction with PIO, which further changed to water-bridge bond with the ligand. Residues Gly98, Phe100, Phe114, Leu208 and Phe476 also tried to interact with the ligand, but the interactions are not stabile.

Docking of NAT over CYP2C9-PIO docked complex. On NAT re-docking over CYP2C9-PIO bound complex, it has been found that the former binding affinity has reduced considerably to −5.8 Kcal/mol from −6.9 Kcal/mol as mentioned before. Allosteric site docking was allowed by plotting the grid box over the whole protein. Thus, it is a plausible approximation that attachment of PIO binding with CYP2C9 changes the conformation of the protein, so that NAT binding affinity goes down on further interaction with the same. From both the drugs docking and dynamics studies, it can be observed that Asn217, which interacted with NAT, also shows a strong and stable interaction with PIO during dynamics.

Discussion

The administration of NAT and PIO together revealed that NAT bioavailability has been increased due to presence of PIO. For example, Pani *et al.* (22) reported that oral administration of single NAT (60 mg) reached a C_{max} of 13.407 µg/mL. Assuming average rabbit blood volume as 112 mL (considering average rabbit weight as 2.0 kg), the bioavailability reached maximally 2.5% in the previous study (22). On the contrary, in the present study, the C_{max} of NAT reached 140.83 µg/mL, assuming average rat weight is 200 g, the bioavailability has been extrapolated to 66.67%. The increase of bioavailability in the study is also supported by increase in $t_{1/2}$ (0.5052 hours), AUC $_{0>\infty}$ and AUMC $_{0>\infty}$ (252.39 µg.h [or h^2]/mL each) in comparison with the data reported by aforementioned authors (0.317 hours, 45.353 µg.h/mL 115.94 µg.h^2/mL, respectively).

Increase in NAT bioavailability may be explained by inhibition of major NAT metabolizing enzymes, such as CYP2C9 and CYP3A4 (24, 25) by PIO. Takanohashi *et al.* 2007 demonstrated that PIO can inhibit CYP2C9 and CYP3A4 with K_i values of 32.1 and 11.8,

Table XII. Pharmacokinetic Parameters of PIO After a Single Oral Dose of 6.16 mg/kg and 1.54 mg/kg PIO and NAT to Three Groups Each Containing 10 Albino Rats

S. No.	Pharmacokinetic parameters	Observed value for NAT
1	Elimination rate constant, k_{el} (h^{-1})	0.40396
2	Time required for maximum plasma concentration, T_{max} (hour)	3
3	Maximum plasma concentration, C_{max} (μg/mL)	27.9002
4	Plasma half-life, $T_{1/2}$ (hour)	1.71589
5	AUC at 24 hours, $AUC_{(0 \rightarrow 24)}$, (μg h/mL)	167.581
6	AUC at infinite time, $AUC_{(0 \rightarrow \infty)}$ (μg h/mL)	167.603
7	Area under momentum curve at 24 hours, $AUMC_{(0 \rightarrow 24)}$ (μg h^2/mL)	911.299
8	Mean residence time, MRT (hour)	5.43796

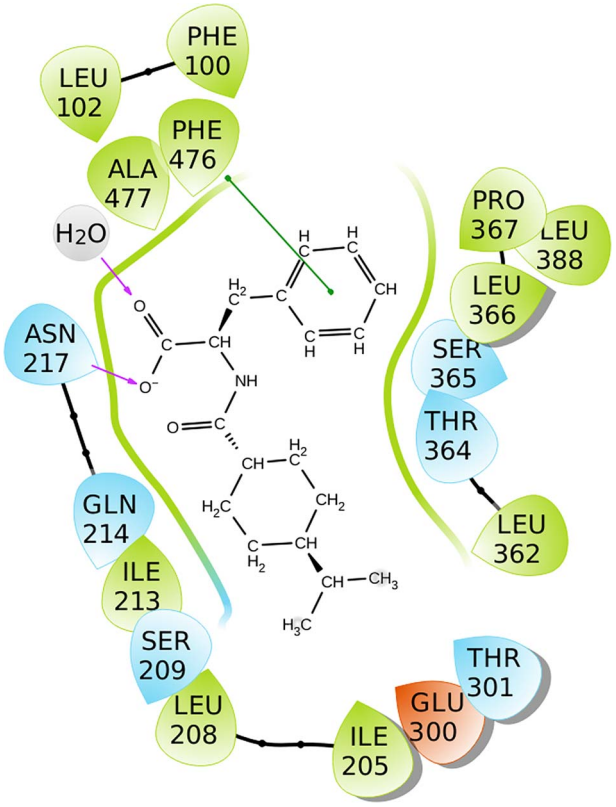

Figure 6. Molecular docking of NAT on solitary CYP3A4.

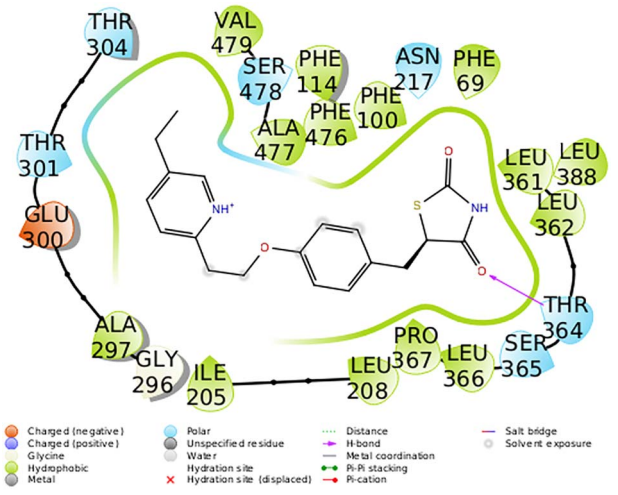

Figure 7. Molecular docking of PIO on solitary CYP3A4.

respectively, with IC_{50} values of 100 and 12.3 μM, respectively (23). The authors also reported that addition of PIO significantly retards the conversion of NAT into its metabolites even with lower risk factor of prolong cytochrome binding.

In pursuit, we have undertaken the study of NAT–PIO interaction in their co-incubation model where metabolism of both the drugs was challenged in their co-incubation system with liver microsomal enzymes and subsequently compared with their individual reaction rates. Earlier reports have demonstrated the plasma estimation of drugs by various methods such as reverse-phase HPLC (20) or LC-MS (21). However, in the former method, the calibration linearity was reported in between 25 and 2000 ng/mL with NAT only, whereas the **limit of detection** (LOD) in our method has been obtained as 15 ng/mL with both NAT and PIO. The latter report again lacked any real-time monitoring of drug concentration in plasma, thus devoid of estimation of any of the pharmacokinetics parameters, whereas our method successfully described pharmacokinetics estimation of certain key parameters of both NAT and PIO with LOD 15 ng/mL and LOQ 50 ng/mL. Not only that but also our method is also comparable with previously reported other methods dedicated on pharmacokinetic or plasma estimation of these two drugs or their metabolites. For example, linearity has been detected as 200–7000 ng/mL (13), while other reports have demonstrated LOD 25 ng/mL (14), linearity 10–50 ng/mL (15), linearity 20–500 ng/mL (16) and linearity 0.5–2000 ng/mL (17, 18). Moreover, these citations reported estimation of solitary drug (either NAT or PIO or their metabolites) is plasma. In comparison, our method has estimated LOD as 15 ng/mL and LOQ 50 ng/mL with simultaneous estimation of both the drugs in rat plasma with concomitant evaluation of all major pharmacokinetic parameters. In addition, our method relying on easy protein precipitation technique with reasonable selectivity and reproducibility is capable for being routinely used for any standard laboratory-based pharmacokinetic estimation of NAT and PIO FDCs. As described earlier, performing this experiment on human beings or any human organs at institute level is prohibited according to regulatory guidelines; thus, we have performed the drug–drug interactions by liver microsomal enzymes using rat liver. It can be seen from the result that when combined NAT and PIO was allowed for conversion by liver microsomal enzymes, the rate of reaction (0.308 U) was decreased to 0.343 times compared with theoretical sum of individual reaction rates of NAT and PIO (0.896 U). First, it suggests that while combined, the compounds play inhibitory roles to each other for metabolic conversion of the same. Second, after 40 seconds interval, the mixed reaction rate decreased even lesser than that of any of the individual drugs. This suggested that one drug may preoccupy the active site of the microsomal enzymes, so that other drug occupation of the same is significantly impaired. This resulted in diminishing its metabolic conversion compared with its solitary reaction rate with the enzymes. The authors' reports also concur with the present pharmacokinetical findings, suggesting that NAT with PIO can be a safe improved choice for

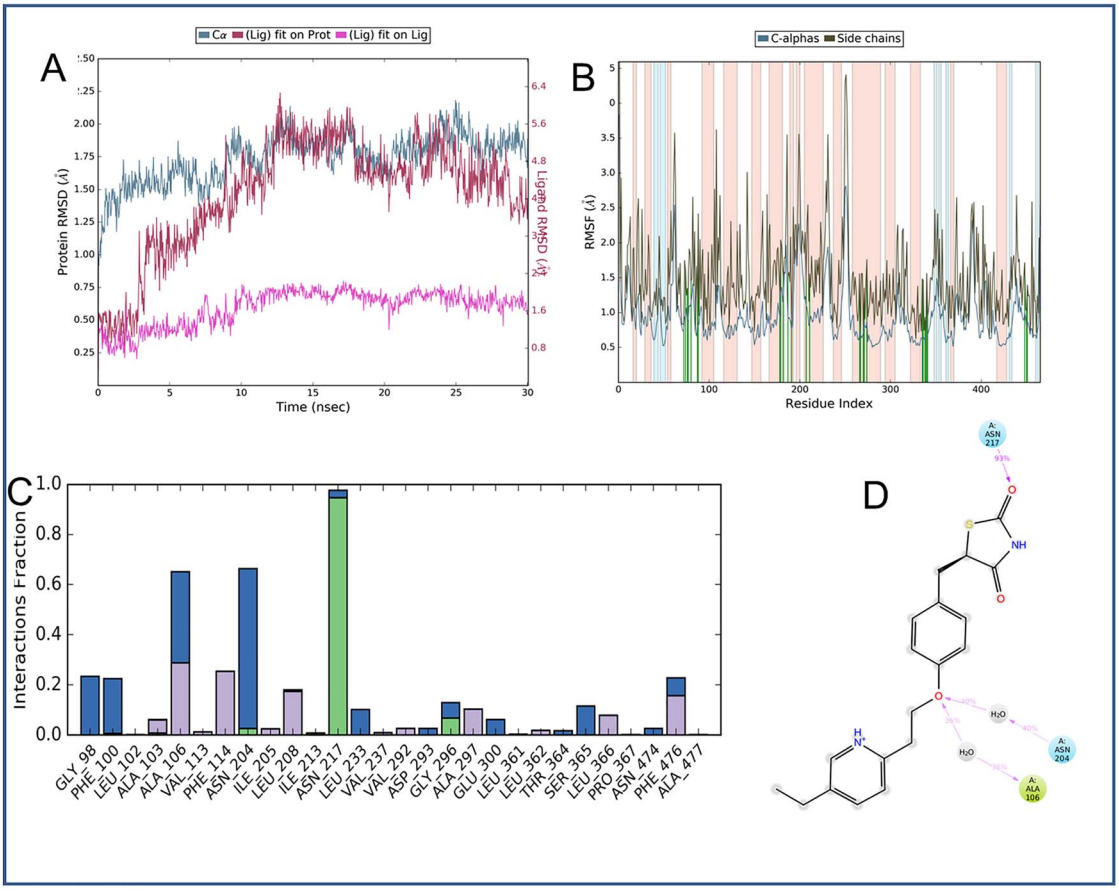

Figure 8. MD simulation of PIO on CYP3A4. (A) RMSD calculation of PIO-CYP3A4 complex; (B) RMSF calculation of PIO-CYP3A4 complex; (C) interaction plot of amino acid residues of the binding site with PIO; (D) different binding interactions of surrounding amino acids with PIO.

antidiabetic therapy with improved bioavailability and higher system retention.

A further insight into the binding chemistry of both the drugs on to CYP2C9 revealed that binding site of both the drugs overlapped greatly with each other. For example, amino acids such as Phe100, Ile205, Leu208, Asn217, Glu300, Thr301, Leu362, Thr364, Ser365, Leu366, Pro367, Leu388, Phe476 and Ala477 have been found common in the binding site for both the drugs. Not only this, a close introspection of the drugs' binding sites revealed that other amino acids which are nonoverlapping also lie within 5–10 amino acid residue distances from each other. Thus, we propose that close interlacing of the drug duo's binding pockets may be the probable reason for drug–drug interaction leading to altered binding of NAT with CYP2C9. CYP2C9 and CYP3A4 have already been acknowledged to catalyze biotransformation of meglitinides (44). These enzymes are well known for drug–drug interaction where one drug metabolism by CYP is inhibited by the other. This is mostly competitive inhibition where one drug occupies the binding site of the other in CYP450 (45), involving both CYP2C9 and CYP3A4, which concurs with the finding of our *in vitro* liver microsomal enzyme inhibition study with NAT and PIO. In addition, organic anion transporting polypeptides (OATP) are also acknowledged to carry the various molecules to CYP450 enzymes in liver. Among them, OATP1B1 (a subfamily of transporter belonging to the class OATP) is mostly responsible to transport NAT from portal circulation to liver microsomal enzymes, thus playing a role also in subsequent biotransformation of NAT (46).

Conclusion

Previously reported HPLC or LC-MS methods for estimating NAT or PIO were based on estimation of the conjugate or FDC of either with any other antidiabetic drug. Moreover, those methods are tedious to tune, involve high technical jargons and may be non-economical due to use of extremely high throughput instrumental counterparts Liquid Chromatography in tandem with Electrospray Ionization Mass Spectrometry (LC-ESI-MS), LC-MS-MS, Ultra-high Performance Liquid Chromatography-Quadrupole Time-of-Flight Mass Spectrometry (UPLC-QToF, MS), which may lead them to be unsuitable for routine analysis in clinical labs. In contrast, the present RP-HPLC based method is accurate, sensitive, simple and economic for the quantitative determination of NAT and PIO in rat plasma. We presume that a LOD of 15 ng/mL together with LOQ of 50 ng/mL fosters considerable sensitivity to the method for fingerprinting traces of drug conjugate in biological matrix. This is the first selective attempt to unlock the combination pharmacokinetics of NAT-PIO FDC, which provides opportunities to dissect any potential drug–drug interaction inside the biological matrix. The preclinical pharmacokinetics study in our work revealed augmented bioavailability of NAT in FDC due to metabolic interaction with PIO (in compliance with earlier report on NAT-PIO-CYP3A4 enzymatic interactions, as described above). On mechanistic investigation of NAT-PIO synergistic interaction *via* MD simulation and molecular docking, the drugs revealed overlapped and close binding pockets

in CYP2C9, which is the chief metabolic enzyme of the drug duo. Furthermore, PIO attachment to the enzyme diminishes affinity of the complex toward further binding with NAT, thus lowering its metabolism and improving its bioavailability. As a whole, this study not only developed a selective, easy high throughput screening method to quantitate the NAT-PIO combination in biological matrix but also unraveled their synergism in a quantitative fashion, so that it could be further exploited for designing dosage form and others.

Supplementary data

Supplementary data available at *Journal of Chromatographic Science* online.

Conflicts of Interest

The authors declare no conflict of interest in submission of this manuscript.

Acknowledgements

The authors are grateful to the Director, Dr S. Chakrabarty, and to the faculty and non-faculty members of the Quality Assurance Department of the Dr. B. C. Roy College of Pharmacy and AHS, Durgapur, West Bengal, India. The authors are also thankful to Mr. Tapan Dutta, Manager, Quality Control, Caplet (India) Pvt. Ltd. for his immense support and provision of infrastructural facilities during initial method development of the work. We also thank the management team for support and for providing chemicals and equipment for this work. We are also thankful to Dr. Reddy's Laboratory, Hyderabad, India, for providing Nateglinide and Lupin Ltd, Goa, India, for providing Pioglitazone, both drugs as gift sample.

References

1. Fujitani, S., Okazaki, K., Yada, T.; The ability of a new hypoglycaemic agent, A-4166, compared to sulphonylureas, to increase cytosolic Ca2+ in pancreatic β-cells under metabolic inhibition; *British Journal of Pharmacology*, (1997); 120(7): 1191–1198.
2. Karara, A.H., Dunning, B.E., McLeod, J.F.; The effect of food on the oral bioavailability and the pharmacodynamic actions of the insulinotropic agent nateglinide in healthy subjects; *The Journal of Clinical Pharmacology*, (1999); 39(2): 172–179.
3. Sohda, T., Momose, Y., Meguro, K., Kawamatsu, Y., Sugiyama, Y., Ikeda, H.; Studies on antidiabetic agents. Synthesis and hypoglycemic activity of 5-[4-(pyridylalkoxy) benzyl]-2, 4-thiazolidinediones; *Arzneimittel-Forschung*, (1990); 40(1): 37–42.
4. Hofmann, C.A., Edwards, C.W. 3rd, Hillman, R.M., Colca, J.R.; Treatment of insulin-resistant mice with the oral antidiabetic agent pioglitazone: evaluation of liver GLUT2 and phosphoenolpyruvate carboxykinase expression; *Endocrinology*, (1992); 130(2): 735–740.
5. Kletzien, R.F., Foellmi, L.A., Harris, P.K., Wyse, B.M., Clarke, S.D.; Adipocyte fatty acid-binding protein: regulation of gene expression in vivo and in vitro by an insulin-sensitizing agent; *Molecular Pharmacology*, (1992); 42(4): 558–562.
6. Sohda, T., Mizuno, K., Momose, Y., Ikeda, H., Fujita, T., Meguro, K.; Studies on antidiabetic agents. 11. Novel thiazolidinedione derivatives as potent hypoglycemic and hypolipidemic agents; *Journal of Medicinal Chemistry*, (1992); 35(14): 2617–2626.
7. Kobayashi, M., Iwanishi, M., Egawa, K., Shigeta, Y.; Pioglitazone increases insulin sensitivity by activating insulin receptor kinase; *Diabetes*, (1992); 41(4): 476–483.
8. Harmel, A.P., Mathur, R.; *Davidson's diabetes mellitus: diagnosis and treatment*. Elsevier Health Sciences, Amsterdam, Netherlands (2004).
9. Krieter, P.A., Colletti, A.E., Doss, G.A., Miller, R.R.; Disposition and metabolism of the hypoglycemic agent pioglitazone in rats; *Drug Metabolism and Disposition*, (1994); 22(4): 625–630.
10. Ono, I., Matsuda, K., Kanno, S.; Determination of N-(trans-4-isopropylcyclohexylcarbonyl)-D-phenylalanine in human plasma by solid-phase extraction and column-switching high-performance liquid chromatography with ultraviolet detection; *Journal of Chromatography B: Biomedical Sciences and Applications*, (1996); 678(2): 384–387.
11. Ono, I., Matsuda, K., Kanno, S.; Determination of N-(trans-4-isopropylcyclohexanecarbonyl)–phenylalanine and its metabolites in human plasma and urine by column-switching high-performance liquid chromatography with ultraviolet detection; *Journal of Chromatography B: Biomedical Sciences and Applications*, (1997); 692(2): 397–404.
12. Ho, E.N., Yiu, K.C., Wan, T.S., Stewart, B.D., Watkins, K.L.; Detection of anti-diabetics in equine plasma and urine by liquid chromatography–tandem mass spectrometry; *Journal of Chromatography B: Analytical Technologies in the Biomedical and Life Sciences*, (2004); 811(1): 65–73.
13. Yan, H., Yang, G., Qiao, F., Chen, Y.; Determination of nateglinide in animal plasma by micellar electrokinetic chromatography and on-line sweeping technique; *Journal of Pharmaceutical and Biomedical Analysis*, (2004); 36(1): 169–174.
14. Zhong, W.Z., Lakings, D.B.; Determination of pioglitazone in dog serum using solid-phase extraction and high-performance liquid chromatography with ultraviolet (229 nm) detection; *Journal of Chromatography B: Biomedical Sciences and Applications*, (1989); 490: 377–385.
15. Yamashita, K., Murakami, H., Teruaki, O., Motohashi, M.; High-performance liquid chromatographic determination of pioglitazone and its metabolites in human serum and urine; *Journal of Chromatography B: Biomedical Sciences and Applications*, (1996); 677(1): 141–146.
16. Zhong, W.Z., Williams, M.G.; Simultaneous quantitation of pioglitazone and its metabolites in human serum by liquid chromatography and solid phase extraction; *Journal of Pharmaceutical and Biomedical Analysis*, (1996); 14(4): 465–473.
17. Lin, Z.J., Ji, W., Desai-Krieger, D., Shum, L.; Simultaneous determination of pioglitazone and its two active metabolites in human plasma by LC–MS/MS; *Journal of Pharmaceutical and Biomedical Analysis*, (2003); 33(1): 101–108.
18. Yin, J., Yang, G., Chen, Y.; Rapid and efficient chiral separation of nateglinide and its l-enantiomer on monolithic molecularly imprinted polymers; *Journal of Chromatography A*, (2005); 1090(1–2): 68–75.
19. Koseki, N., Kawashita, H., Niina, M., Nagae, Y., Masuda, N.; Development and validation for high selective quantitative determination of metformin in human plasma by cation exchanging with normal-phase LC/MS/MS; *Journal of Pharmaceutical and Biomedical Analysis*, (2005); 36(5): 1063–1072.
20. Pani, N.R., Nath, L., Singh, A.V., Mahapatra, S.K.; Development and validation of analytical method for the estimation of nateglinide in rabbit plasma; *Journal of Pharmaceutical Analysis*, (2012); 2(6): 492–498.
21. Wang, M., Miksa, I.R.; Multi-component plasma quantitation of anti-hyperglycemic pharmaceutical compounds using liquid chromatography–tandem mass spectrometry; *Journal of Chromatography B: Analytical Technologies in the Biomedical and Life Sciences*, (2007); 856(1–2): 318–327.
22. Holstein, A., Beil, W., Kovacs, P.; CYP2C metabolism of oral antidiabetic drugs - impact on pharmacokinetics, drug interactions and pharmacogenetic aspects; *Expert Opinion in Drug Metabolism and Toxicology*, (2012); 8(12): 1549–1563.
23. Takanohashi, T., Koizumi, T., Mihara, R., Okudaira, K.; Prediction of the metabolic interaction of nateglinide with other drugs based on *in vitro* studies; *Drug Metabolism and Pharmacokinetics*, (2007); 22(6): 409–418.
24. Guardado-Mendoza, R., Prioletta, A., Jiménez-Ceja, L.M., Sosale, A., Folli, F.; The role of nateglinide and repaglinide, derivatives of meglitinide, in the treatment of type 2 diabetes mellitus; *Archives of Medical Science: AMS*, (2013); 9(5): 936.

25. Weaver, M.L., Orwig, B.A., Rodriguez, L.C., Graham, E.D., Chin, J.A., Shapiro, M.J. *et al.*; Pharmacokinetics and metabolism of nateglinide in humans; *Drug Metabolism and Disposition*, (2001); 29(4): 415–421.
26. Chhetri, H.P., Thapa, P., Van Schepdael, A.; Simple HPLC-UV method for the quantification of metformin in human plasma with one step protein precipitation; *Saudi Pharmaceutical Journal*, (2014); 22(5): 483–487.
27. Helmy, S.A., El Bedaiwy, H.M.; A new and simple HPLC method for determination of etamsylate in human plasma and its application to pharmacokinetic study in healthy adult male volunteers; *Saudi Pharmaceutical Journal*, (2013); 21(4): 405–410.
28. Mowafy, H.A., Alanazi, F.K., El Maghraby, G.M.; Development and validation of an HPLC–UV method for the quantification of carbamazepine in rabbit plasma; *Saudi Pharmaceutical Journal*, (2012); 20(1): 29–34.
29. Anonymous; US Food and Drug Administration, Center for Drug Evaluation and Research (CDER); *Analytical method validation, guidance for the industry*, Rockville, MD, (2000).
30. Anonymous; International Conference on Harmonization (ICH); *Validation of analytical procedures: text and methodology Q2 (R1)*, Geneva, Switzerland, (2005).
31. Anonymous; International Conference on Harmonization (ICH); Guidance for industry: Q2B validation of analytical procedures: Methodology. Food and drug administration, centre for drug evaluation and research; *Centre for Biologics Evaluation and Research*, (1996) .
32. Bradford, M.M.; Rapid and sensitive method for the quantification of microgram quantities of protein utilizing the principle of protein-dye binding; *Analytical Biochemistry*, (1976); 72(1–2): 248–254.
33. Ramar, V., Pappu, S.; Exploring the inhibitory potential of bioactive compound from Luffa acutangula against NF-κB—a molecular docking and dynamics approach; *Computational Biology and Chemistry*, (2016); 62: 29–35.
34. Brändén, G., Sjögren, T., Schnecke, V., Xue, Y.; Structure-based ligand design to overcome CYP inhibition in drug discovery projects; *Drug Discovery Today*, (2014); 19(7): 905–911.
35. Taha, M.O., Habash, M., Al-Hadidi, Z., Al-Bakri, A., Younis, K., Sisan, S.; Docking-based comparative intermolecular contacts analysis as new 3-D QSAR concept for validating docking studies and in silico screening: NMT and GP inhibitors as case studies; *Journal of Chemical Information and Modeling*, (2011); 51(3): 647–669.
36. Sastry, G.M., Adzhigirey, M., Day, T., Annabhimoju, R., Sherman, W.; Protein and ligand preparation: parameters, protocols, and influence on virtual screening enrichments; *Journal of Computer-aided Molecular Design*, (2013); 27(3): 221–234.
37. Bas, D.C., Rogers, D.M., Jensen, J.H.; Very fast prediction and rationalization of pKa values for protein–ligand complexes; *Proteins: Structure, Function, and Bioinformatics*, (2008); 73(3): 765–783.
38. Li, H., Robertson, A.D., Jensen, J.H.; Very fast empirical prediction and rationalization of protein pKa values; *Proteins: Structure, Function, and Bioinformatics*, (2005); 61(4): 704–721.
39. Mustyala, K.K., Malkhed, V., Chittireddy, V.R., Vuruputuri, U.; Virtual screening studies to identify novel inhibitors for Sigma F protein of Mycobacterium tuberculosis; *International Journal of Mycobacteriology*, (2015); 4(4): 330–336.
40. Tyagi, C., Gupta, A., Goyal, S., Dhanjal, J.K., Grover, A.; Fragment based group QSAR and molecular dynamics mechanistic studies on arylthioindole derivatives targeting the α-β interfacial site of human tubulin; *BMC Genomics*, (2014); 15(9): S3.
41. Pradeepkiran, J.A., Kumar, K.K., Kumar, Y.N., Bhaskar, M.; Modeling, molecular dynamics, and docking assessment of transcription factor rho: a potential drug target in Brucella melitensis 16M; *Drug Design, Development and Therapy*, (2015); 9: –1897.
42. Kallubai, M., Amineni, U., Mallavarapu, M., Kadiyala, V.; In silico approach to support that p-nitrophenol monooxygenase from Arthrobacter sp. strain JS443 catalyzes the initial two sequential monooxygenations; *Interdisciplinary Sciences: Computational Life Sciences*, (2015); 7(2): 157–167.
43. Meyyanathan, S.N., Ramasarma, G.V.S., Suresh, B.; Analysis of simvastatin in pharmaceutical preparations by high performance thin layer chromatography; *ARS Pharmaceutica*, (2004); 45(2): 121–129.
44. Kirchheiner, J., Roots, I., Goldammer, M., Rosenkranz, B., Brockmoller, J.; Effect of genetic polymorphisms in cytochrome P450 (CYP) 2C9 and CYP2C8 on the pharmacokinetics of oral antidiabetic drugs; *Clinical Pharmacokinetics*, (2005); 44(12): 1209–1225.
45. Bibi, Z.; Role of cytochrome P450 in drug interactions; *Nutritional Metabolism (London)*, (2005); 5: 27.
46. Maideen, N.M.P., Manavalan, G., Balasubramanian, K.; Drug interactions of meglitinide antidiabetics involving CYP enzymes and OATP1B1 transporter; *Therapeutic Advances in Endocrinology and Metabolism*, (2018); 9(8): 259–268.